# LASER INTERFEROMETER GRAVITATIONAL WAVE OBSERVATORY
## -LIGO-
California Institute of Technology
Massachusetts Institute of Technology

---

Document Number: **LIGO- T020147-00-R**   Date:   10/1/02

Authors: **David Bonfield** , Ben Abbott, Osamu Miyakawa,
Dennis Ugolini, Alan Weinstein, Steve Vass

---

## Characterizing the length sensing and control system of the mode cleaner in the LIGO 40m lab

---

*This is an internal working note*
*of the LIGO Laboratory.*

# Characterizing the length sensing and control system of the mode cleaner in the LIGO 40m lab.

## David Bonfield

Cambridge University
Mentor – Alan Weinstein
LIGO SURF program, 2002

## *Table of Contents*

## *Table of Figures*

## 1 – Abstract

The LIGO project aims to build the world's first large (km) scale detectors of gravitational waves. The 40m lab is designed to prototype a number of systems to be used in Advanced LIGO, the second generation of LIGO interferometers, and is being upgraded with a 13 meter mode cleaner cavity to produce a highly stable laser beam. I have characterised the components of the systems that control the length of the cavity and stabilise the laser frequency. The transfer functions of part of the control loop were measured and found to be consistent with models, though electronics faults prevented the mode cleaner from locking in its design configuration. The DC response of the VCO was measured. The finesse, visibility and length of the mode cleaner cavity were measured. The spectrum of the residual frequency noise in the laser beam (with respect to the mode cleaner resonance) was measured and compared with the design requirement. The intensity stability and transverse profile of the beam passed by the mode cleaner were measured.

## 2 – Introduction

### 2.1 – Motivation for LIGO

General relativity predicts that massive accelerating objects will cause oscillating distortions of space-time, which propagate as waves from the source.  LIGO – the Laser Interferometer Gravitational-Wave Observatory, aims to detect such waves[1,2].

The motivation for LIGO is the information that will be gained by studying the gravitational waves from expected (and hopefully unexpected) sources.  Predicted sources include black hole and neutron star binary inspirals, asymmetric supernovae and pulsars, and possibly signatures from the beginnings of the universe as early as $10^{-34}$ seconds after the big bang.

### 2.2 – Detecting Gravitational Waves

As a gravitational wave propagates, it causes objects that it passes through to be stretched and compressed in perpendicular directions.  LIGO aims to detect this by measuring the difference in strain in two perpendicular arms of a laser interferometer.  Each arm is a Fabry-Perot cavity 4 km in length.  (Using Fabry-Perot cavity arms effectively increases the path length by a factor of about 50, and thus increases the strain sensitivity.)

### 2.3 – Advanced LIGO and the Caltech 40-meter lab

As currently built, (Initial) LIGO will only be capable of detecting events that are either very close by or extremely violent.  The second-generation detector, Advanced LIGO, aims to increase the sensitivity of LIGO by a factor of 10, enabling sources to be detected in a volume of space $10^3$ times as large.

The optical configuration and control systems for Advanced LIGO (Figure 1) are to be tested at the 40-meter prototype laboratory at Caltech.  The current focus of work is the input optics system, whose purpose is to deliver a laser beam of sufficiently stability (in frequency, intensity, position and angle) into the interferometer.  The main components of this system are a pre-stabilized laser (PSL), a 13-meter suspended-mass mode cleaner (MC) and the control systems associated with these (described in more detail below).  There are also mode-matching telescopes to ensure that the transverse mode defined by each cavity is matched to the mode of the next cavity.

## 2.4 – Purpose of the present work

Over the ten weeks I spent at Caltech, my task was to characterize, as fully as possible, the performance of the mode cleaner and its control systems. The overall goal of this task would be to check that, once fully commissioned, the mode cleaner performed as laid down in specification documents. Ultimately, it is required to pass a laser beam of the same quality as its counterparts at the Hanford and Livingston observatories. The specific qualities required are discussed in the next section.
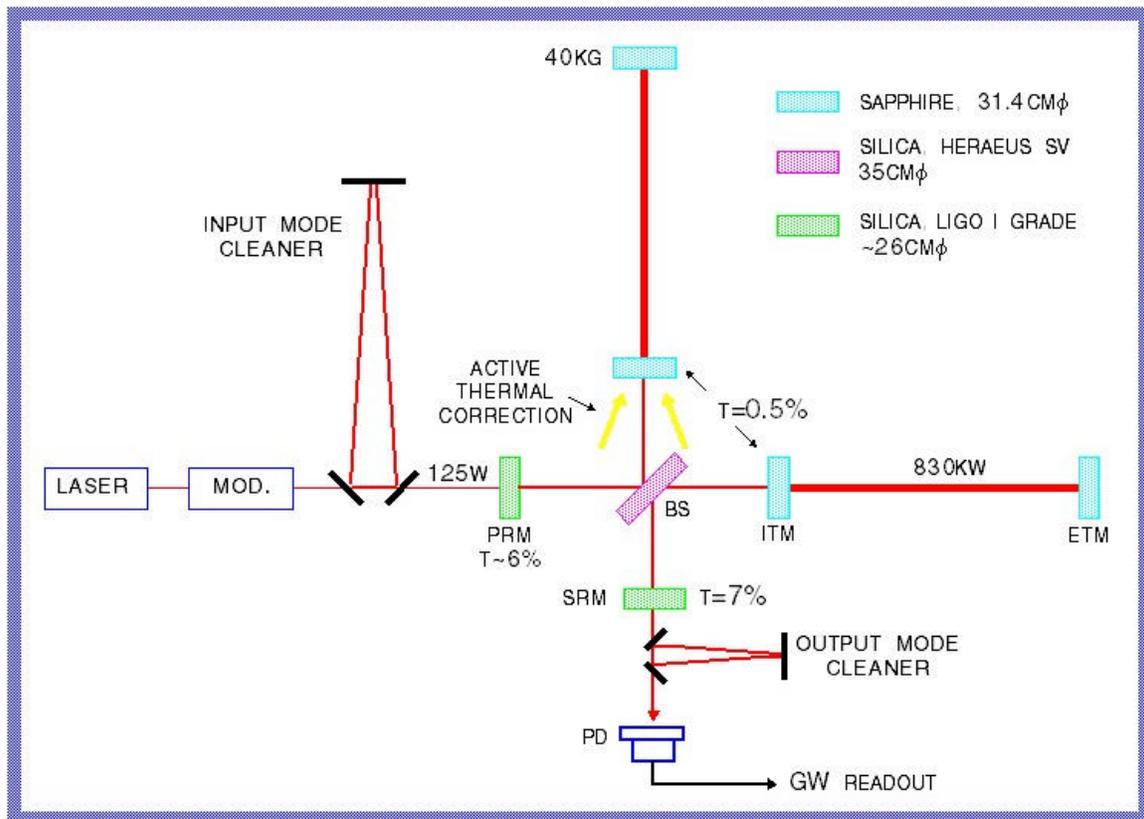


**Figure 1: The Advanced LIGO proposed configuration.**

## 3 – The Mode Cleaner

### 3.1 – Construction

The mode cleaner is a triangular Fabry-Perot cavity, 13.5 meters in half-length (half the round-trip optical path), whose purpose is to further stabilize the beam from the PSL. The mode cleaner mirrors (denoted MC1, MC2 and MC3 as shown in Figure 2) are suspended on loops of wire in a vacuum to isolate them from high frequency noise as far as possible. (The suspension points are themselves on passive seismic isolation stacks consisting of a series of large masses and damped springs). This is so that the mode cleaner's resonant frequency is more stable than the laser frequency against high frequency fluctuations.
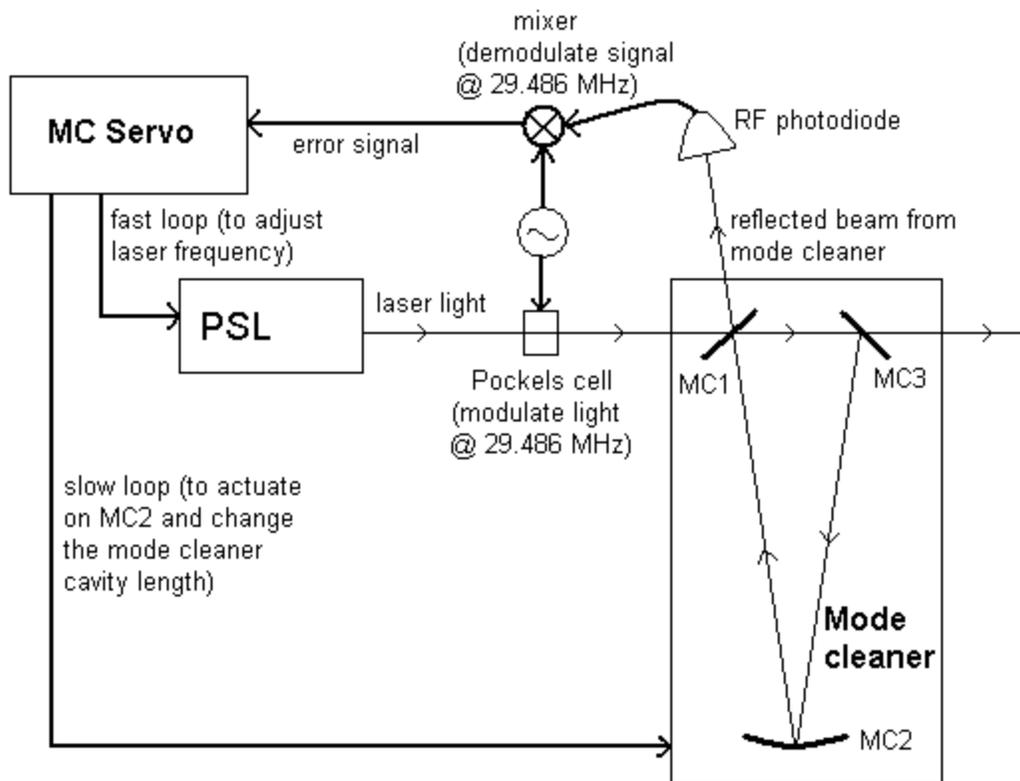


**Figure 2: Overview of the modecleaner-based frequency stabilization scheme.**

### 3.2 – Optical properties

A small number of the physical parameters of the mode cleaner can be used to derive its optical properties and the characteristics of the beam that resonates in it. As an exercise in understanding the optical properties of the mode cleaner, I have calculated the free spectral range, finesse, storage time, cavity pole, beam waist size, Rayleigh length, beam divergence angle and the spot sizes on the mirrors. **These calculations are based on design specifications and NOT measurements.**

To perform these calculations we need know only the following independent parameters:

- The half-length, $L$, of the cavity – designed to be 13.542 meters. (Note that this is half the round-trip length of the triangular cavity.)
- The (amplitude) reflectivities of the mirrors, $r_{mc1}$, $r_{mc2}$ and $r_{mc3}$. Transmittances (of power) of the mirrors are laid down in design documents (0.00001 for MC2 and 0.002 for MC1 and MC3), so I have assumed the reflectance of each mirror is 1, less the transmittance and the loss in the mirror. The loss due to scatter and absorption of light for the whole mode cleaner has been described several times[3] as 50 ppm, and so I have approximated the loss per mirror to be 15 ppm. This gives:

$$r_{mc1} = r_{mc3} = 0.998991991...$$

$$r_{mc2} = 0.999987499...$$

- The radius of curvature, $R$, of the curved mirror (MC2), which is specified in terms of the quantity $g$, given by

$$g = 1 - \frac{L}{R}$$

since $g$ is the quantity which determines the stability of the cavity (stable for $g < 1$) and the relative transmittances of different TEM modes. The value of $g$ specified is 0.36153. (For this value of $g$, the transmissions of the first 20 higher order modes are expected to be less than $10^{-4}$ that of the $TEM_{00}$ mode[4].) This corresponds to $R = 21.210$ m.

- The wavelength, $\mathit{l}$, of the laser: 1064 nm.

## 3.2.1 – Free spectral range

The free spectral range (FSR) of the cavity is the separation in frequency space of adjacent allowed resonances. The separation of resonances in length is, for a ring cavity, equal to the wavelength of light. Since

$$\frac{\Delta f}{f} = \frac{\Delta l}{l},$$

we can identify the FSR as $\Delta f$, the round-trip length ($2L$) as $l$ and the wavelength of the light as $\Delta l$ to give:

$$FSR = f \frac{\mathit{l}}{2L} = \frac{c}{\mathit{l}} \frac{\mathit{l}}{2L} = \frac{c}{2L}$$

where $c$ is the speed of light *in vacuo*. Hence,

$$FSR = 11.069 \text{ MHz.}$$

### 3.2.2 - Finesse

Finesse is the ratio of the free spectral range to the width of a resonant peak (in frequency space). This can be calculated from the reflectivities of the mirrors. For the mode cleaner,

$$Finesse = \boldsymbol{p}\,\frac{\sqrt{r_{mc1}r_{mc2}r_{mc3}}}{1 - r_{mc1}r_{mc2}r_{mc3}}$$
$$= 1548$$

### 3.2.3 – Storage time

The mean number of round-trips that a resonant beam makes before being transmitted is equal to the finesse divided by pi. Thus, the mean storage time, $\boldsymbol{t}$, of light circulating in the mode cleaner is given by

$$\boldsymbol{t} = \frac{Finesse}{\boldsymbol{p}}\frac{2L}{c}$$
$$= 44.5\,\boldsymbol{m}s$$

### 3.2.4 – Cavity pole

A result of the storage of light in the mode cleaner is that it acts as an optical low-pass filter, with a single pole at $f_{pole}$, referred to as the 'cavity pole'. This filter should passively attenuate high frequency fluctuations in frequency and intensity. By a similar process the mode cleaner helps reject beam position and angle fluctuations.

$$f_{pole} = \frac{1}{2\boldsymbol{p}\boldsymbol{t}}$$
$$= 3575\,\text{Hz}$$

### 3.2.5 – Beam waist

The waist of the resonant beam lies between MC1 and MC3, equidistant from the nearest two images of (the curved mirror) MC2. The width at the waist, $w_0$, expressed as the radius at which the amplitude drops to $1/e$ its maximum value, can be calculated directly from $g$:

$$w_0 = \left(\frac{\boldsymbol{l}L}{\boldsymbol{p}}\sqrt{\frac{g}{1-g}}\right)^{1/2}$$
$$= 1858\,\boldsymbol{m}\text{m}$$

### 3.2.6 – Rayleigh length

The Rayleigh length, $z_R$, is the distance the beam has traveled away from its waist for its diameter to increase by a factor of $\sqrt{2}$.

$$z_R = \frac{p w_0^2}{l}$$
$$= 10.19 \text{ m}$$

### 3.2.7 – Divergence angle

In the far field (i.e. for distances much greater than the Rayleigh length), the hyperbolic curve which the beam width follows is very close to its asymptotes. Since these are straight lines, the beam width (defined as in **3.2.5**) can be thought of as having a constant divergence angle from its axis, $q$. The total divergence of the beam is given by

$$2q = \frac{2l}{p w_0}$$
$$= 182 \text{ } m\text{rad}$$

### 3.2.8 – Propagation of the beam

At a general distance $z$ from the beam waist, the width, $w_z$, of the beam is given by

$$w_z = w_0 \sqrt{1 + \left(\frac{z}{z_R}\right)^2}$$

By 'width' we mean, again, the radius at which the amplitude falls to $1/e$ its maximum value.

This is useful, for example, in determining the spot sizes on the mirrors. We can convert from the 'width', $w_z$, to the diameter, $d$, at which only 1 ppm of power is excluded by integrating over the Gaussian transverse profile of the beam to give:

$$d = 2\sqrt{-\frac{w_z^2}{2} \ln\left(10^{-6}\right)}$$

For MC1 and MC3, $d = 9.77$ mm. For MC2, $d = 16.24$ mm.

### 3.2.9 – Visibility

By considering the interference of light amplitudes at MC1 and MC3, it can be shown[5] that the reflected amplitude $E_r$ is given by

$$E_r = E_i \left( \frac{r_{MC1} + \left(r_{MC1}^2 + t_{MC1}^2\right) r_{MC2} r_{MC3} e^{-2ikL}}{1 + r_{MC1} r_{MC2} r_{MC3} e^{-2ikL}} \right)$$

where $E_i$ is the incident ampltitude, $t_{MC1}$ is the amplitude transmission coefficient of MC1 and $k$ is the wavevector. In resonance, $2kL$ is an integral multiple of $2\boldsymbol{p}$. In anti-resonance, $2kL$ is an odd multiple of $\boldsymbol{p}$. Thus we can predict the maximum and minimum power (equal to amplitude squared) values, $P_{max}$ and $P_{min}$, for light reflected by the mode cleaner, and hence the visibility, $V$, for a perfectly aligned and mode-matched mode cleaner at a pure frequency:

$$V = \frac{P_{\max} - P_{\min}}{P_{\max} + P_{\min}}$$
$$= 0.99963$$

## 3.3 – Locking the mode cleaner to optical resonance

The deviation of the mode-cleaner from optical resonance is determined by Pound-Drever-Hall reflection locking[6]. Frequency sidebands are placed on the carrier light by a Pockels cell modulated at 29.486 MHz. This frequency is chosen so that it is not transmitted through the mode cleaner when this is locked to the carrier, but is instead reflected to a radio frequency photodiode (RFPD). The signal from the RFPD is demodulated at 29.486 MHz to produce an error signal proportional to the imaginary amplitude component of the carrier light reflected from the mode cleaner (see Figure 2).

When the mode-cleaner cavity is close to perfect resonance, termed 'in lock', this error signal is linearly related to the deviation in frequency (of the laser) or length (of the mode-cleaner) and gives the amplitude and sign of the required correction. The error signal is filtered by the "mode cleaner servo" circuit board. High frequency components of the error signal are used to correct the laser frequency. Low frequency components are used to stabilize the mode cleaner length (which is less stable than the laser at low frequencies) by driving "OSEM" magnetic actuators. The OSEMs sense the position of the suspended optic relative to its suspension cage using an LED and photodiode shadow sensor.
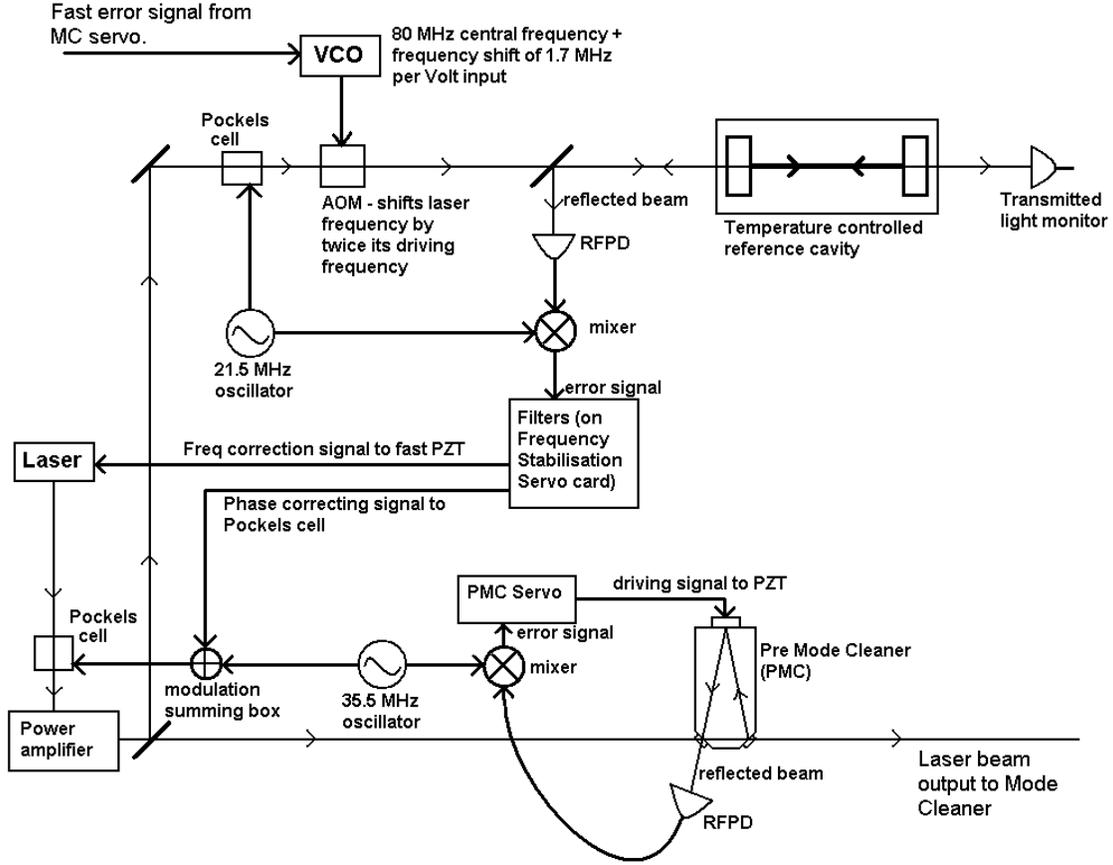
**Figure 3: Details of the frequency stabilization control loops within the PSL (pre-stabilised laser).**

The PSL is itself locked, by a similar method, to a temperature-controlled reference cavity, 20 cm in length (see Figure 3). In both cases, the frequency feedback signal to the laser is proportional to the fluctuation in phase difference, $df$, between the laser and the resonance of the cavity, with

$$df = d\left(\frac{4pLf}{c}\right) = \frac{4pf}{c}dL + \frac{4pL}{c}df \qquad [1]$$

where $df$ is the laser frequency fluctuation, $dL$ is the fluctuation in the length of the cavity and $c$ is the speed of light. The frequency noise suppression can only be effective when the second term in the above expansion of $df$ dominates, i.e. when $Ldf > fdL$. This implies that the smallest laser frequency fluctuation that can be compensated for is given by

$$df_{min} \approx \frac{dL}{L}f \,. \qquad [2]$$

Since the mode cleaner is around 100 times longer than the PSL reference cavity, with mirror suspensions that should be about 10 times more stable, we expect the mode cleaner to deliver a laser beam around 1000 times more stable than the PSL, meeting the design requirement[7] shown in Figure 4.
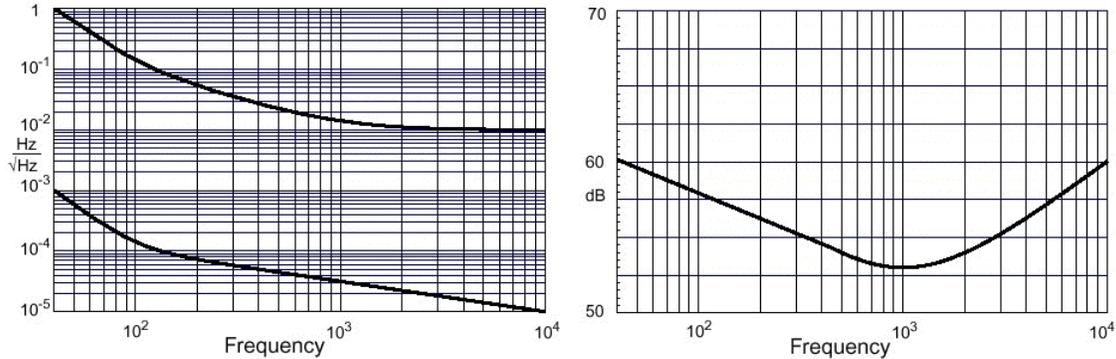


**Figure 4: Left - Frequency fluctuation requirements for the beams delivered by the PSL (top) and mode cleaner (bottom). Right - The corresponding level of noise suppression that the mode cleaner must provide.**

## 3.4 – The control loop

The path of the control signal feeding back on the laser is shown in Figure 3. After being filtered and amplified by the mode cleaner servo the signal is sent to the VCO, a voltage-controlled oscillator, which sends an 80MHz signal, shifted by an amount proportional to its input voltage, to a double-pass acousto-optic modulator (AOM). The AOM causes the laser frequency to be shifted by twice the frequency it is driven at. After passing through the AOM the light is sent to the reference cavity, which is kept in lock by the frequency stabilization servo (FSS). The FSS sends signals to three actuators to change the laser frequency: the slow actuator (not shown) changes the temperature of the laser, the fast actuator is a PZT on the end of the laser cavity that changes its length, and phase corrections are applied using a Pockels cell.

The length control signal path is very different, with most of the signal processing performed digitally. Figure 5 shows a block diagram of the signal's path through the various electronic modules. The Pentium CPU is responsible for adding the length control signal to a damping signal that aims to critically damp the optics. The positions and orientations of the optics are monitored by the OSEM shadow sensors (see Figure 6[8]), and controlled using the OSEMs' magnetic coils.
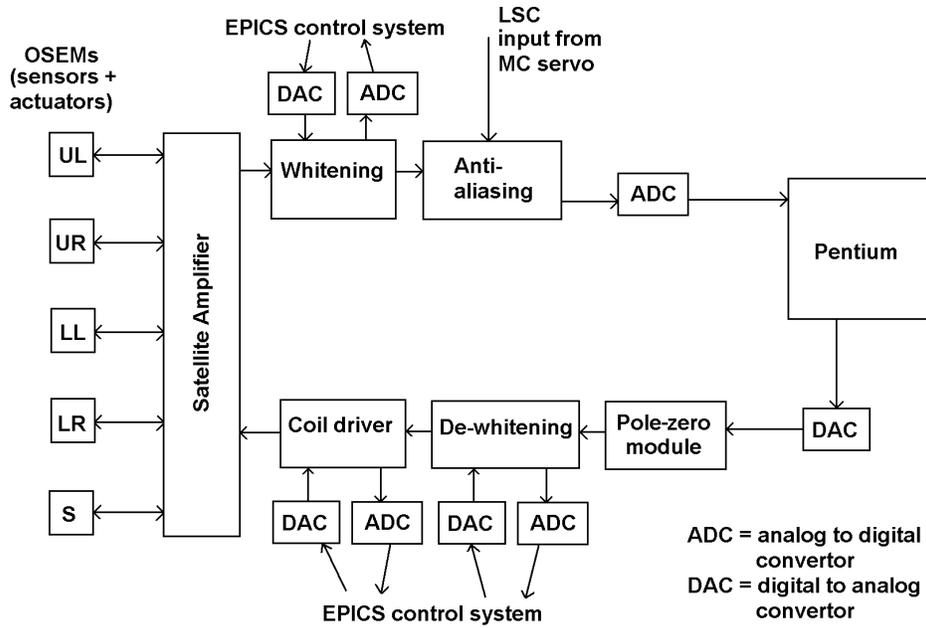
**Figure 5: The path of the mode cleaner length control signal from the MC servo to the OSEMs.**
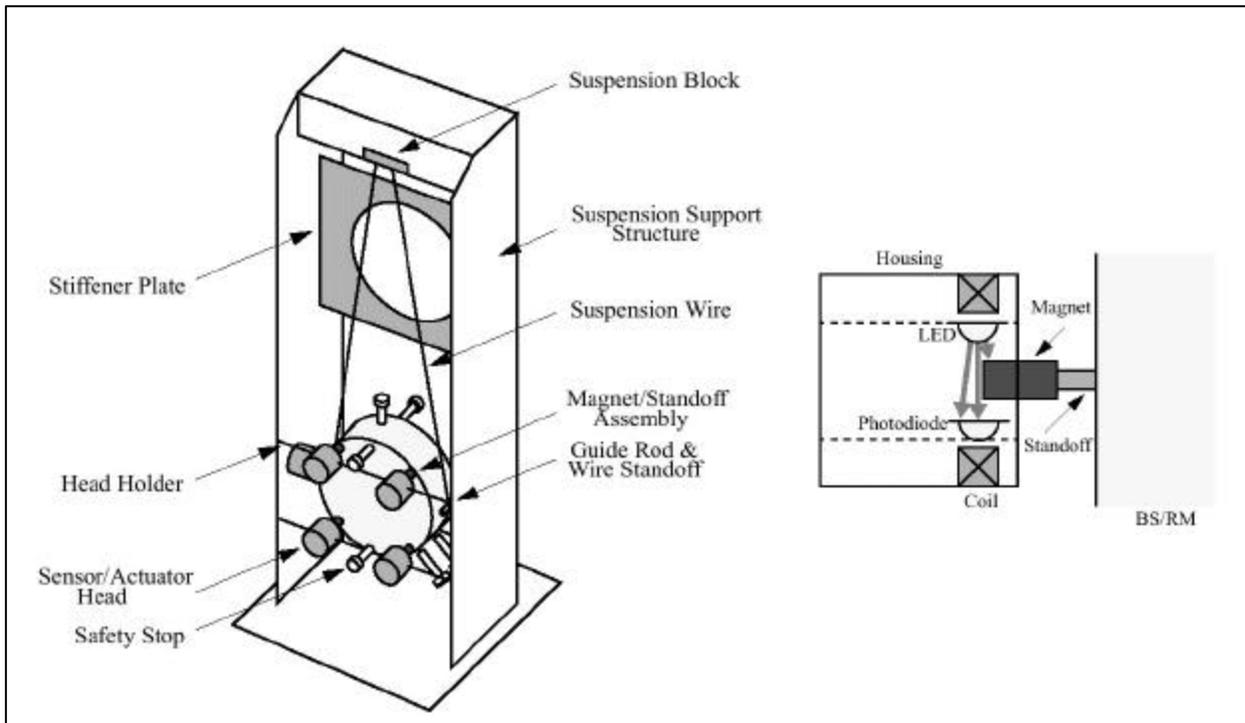


**Figure 6: Left - A suspended mirror, showing the positions of the 5 OSEM sensor/actuators.  Right - A cross-section through an OSEM.**

Figure 7 shows a block diagram of the control system, with the *expected* response of each block in terms of the poles and zeroes of its transfer function:

- $E_{paf}$ is the preliminary amplification and filtering of the error signal on the MC servo card.
- $E_l$ is the further filtering of the signal sent to correct the laser frequency, where the first three pole-zero pairs are filters on the MC servo and the last pair (pole at 1.6 Hz, zero at 40 Hz) is a filter in the VCO box.
- $H_l$ includes the transfer functions of the VCO and the AOM (which convert the voltage applied into a frequency shift of the laser) as well as the filtering of the light due to the pre-mode cleaner and the effect of the frequency stabilization servo (FSS).
- $E_m$ represents the transfer function of the additional electronics in the mirror actuation path, including the MC servo card, the dewhitening board (elliptic filter), the software filters in the Pentium and the pole-zero module. The coil drivers each also have a pole at 1 Hz and a zero at 40 Hz, but this is compensated for and cancelled out in software filters.
- $H_m$ is the transfer function of the mirror treated as a damped pendulum (although the damping is in practice carried out actively). The value of 1.4 microns per Volt is taken from the design document[9] – Ilya Berdnikov (a fellow SURF student), measured the response of the coils of MC2 (the optic which is actuated on to control the mode cleaner length) to range from 3.28 to 3.77 microns per Volt at DC[10].
- $X_{mc}$ is the conversion factor from the length fluctuations of the mode cleaner to a frequency fluctuation, equal to the ratio of the laser frequency to the mode cleaner length.
- $C_{mc}$ is the optical filtering due to the mode cleaner's cavity pole
- $D_{mc}$ represents the conversion of the frequency difference between the laser and the mode cleaner resonance into a voltage, and includes the photodiode transfer function, the depth of the RF modulation, etc. The figure shown is for the Hanford 2 km interferometer
- $L_{mc}$, $F_{psl}$ and $V_s$ represent the MC length noise, the PSL frequency noise and the photodetector sensor noise respectively.
- $G$ is an amplifier that I added along with test input and output $V_{in}$ and $V_{out}$ for the purpose of taking a closed loop transfer function. All three of these would be temporary parts of the control system and can be ignored, especially since I was unable to successfully measure this transfer function.
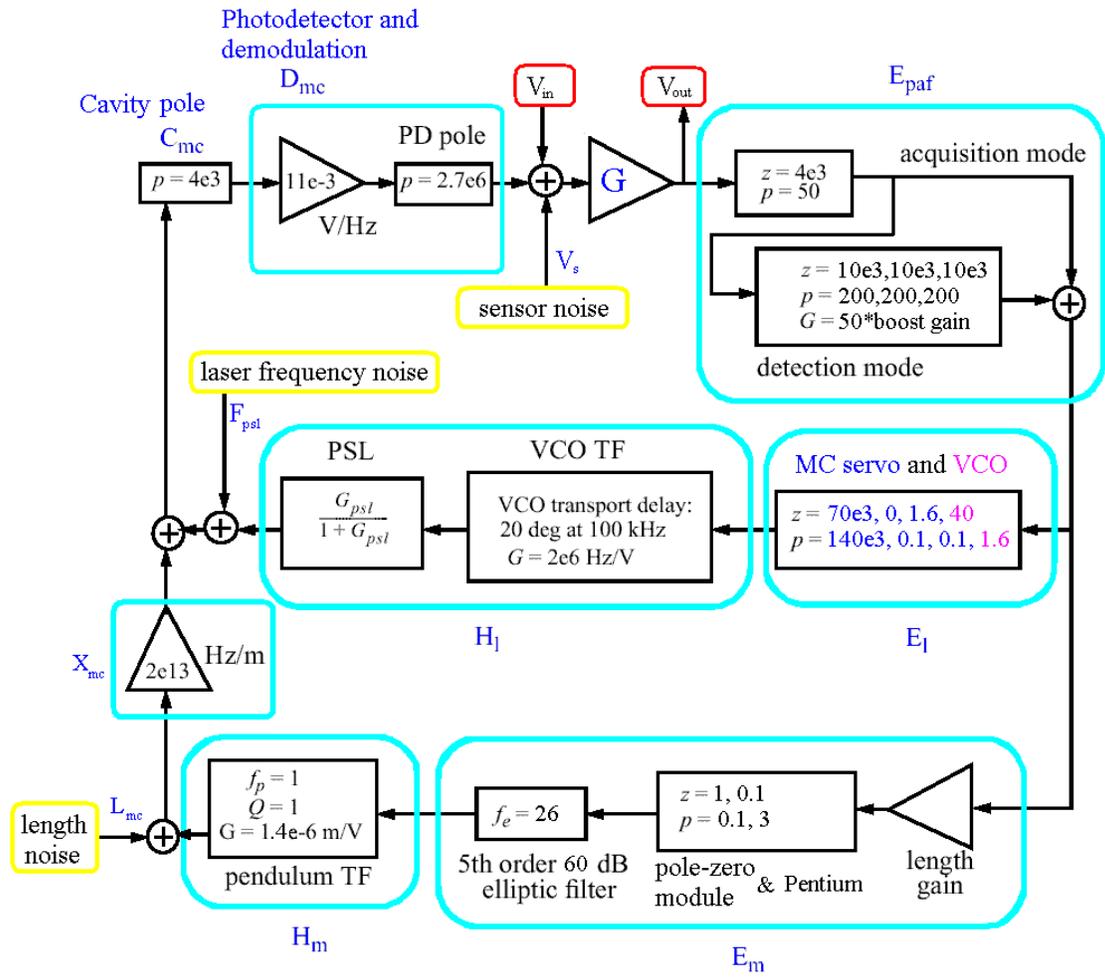
**Figure 7: A block diagram of the mode cleaner frequency stabilization loop, based on numbers from design documents.**

## *4 – Measurements*

Most of the optical characteristics of the mode cleaner are best measured, and in some cases can only be measured, when it is in lock. For the majority of the time I was working in the 40m lab, we were unable to lock the mode cleaner. The reasons for this were not fully understood at the time: they are now known to have been errors in the electronics caused by out-of-date schematics and assembly errors. As a result, I began my work characterizing the electronic systems that were straightforward to measure without locking the mode cleaner. I hoped that I would be able to help diagnose problems in the system, by comparing the behavior of portions of the system with the design.

It is worth noting that whilst I was taking measurements of the electronic systems, and even after I had left the lab, modifications were being made to them (in particular the MC servo board). Accordingly, data should not necessarily be taken as representative of the final configuration of the system.

Towards the end of the summer, in an effort to better explain the mode cleaner's failure to lock, Osamu replaced the operation of the MC servo board with a number of SR560 Stanford pre-amplifiers. By carefully choosing the gains and filtering applied to the error signals passed to the laser and mirror feedback mechanisms, this set-up allowed the mode cleaner to achieve stable lock.

While the mode cleaner was locked in this way a number of the optical properties were measured, namely the finesse (section **4.4**), the transverse beam profile (**4.6**) and the visibility (**4.7**). I also took a power spectrum of the error signal to give a measure of the residual frequency noise in the laser (**4.3**) and examined the intensity stability of the beam delivered by the mode cleaner (**4.5**). The length of the mode cleaner was accurately measured later (**4.8**).

## 4.1 – Transfer functions

Transfer functions of several components of the system were measured using an HP3563 network analyzer. This device can measure the response of any linear system (with electronic inputs and outputs) by recording the gain and phase delay of a sine wave, which it supplies to an actuator in the system while sweeping the frequency of the sine wave.

### 4.1.1 – The mode cleaner servo

This circuit board performs some of the filtering and much of the amplification to the control signals sent to the laser and mode cleaner mirror actuators. It was easy to connect the HP3563 to the board to measure its transfer functions, but I was unable to find a document specifying what should be expected. For comparison with my measurements, I

used the circuit diagrams [11] to construct models using MATLAB. I was then able to compare the shapes of the magnitude and phase responses as a function of frequency.

The model I constructed focused on the shape of the response curves and not the absolute magnitude. I adjusted the overall magnitude of the models to fit the data in order to more easily notice deviations from my models.

Figure 8 shows measured and modeled transfer functions for the length path (i.e. that to the mirror actuator) of the MC servo, when in acquisition mode. The model includes the poles and zeros shown in Figure 7 in block $E_{paf}$.
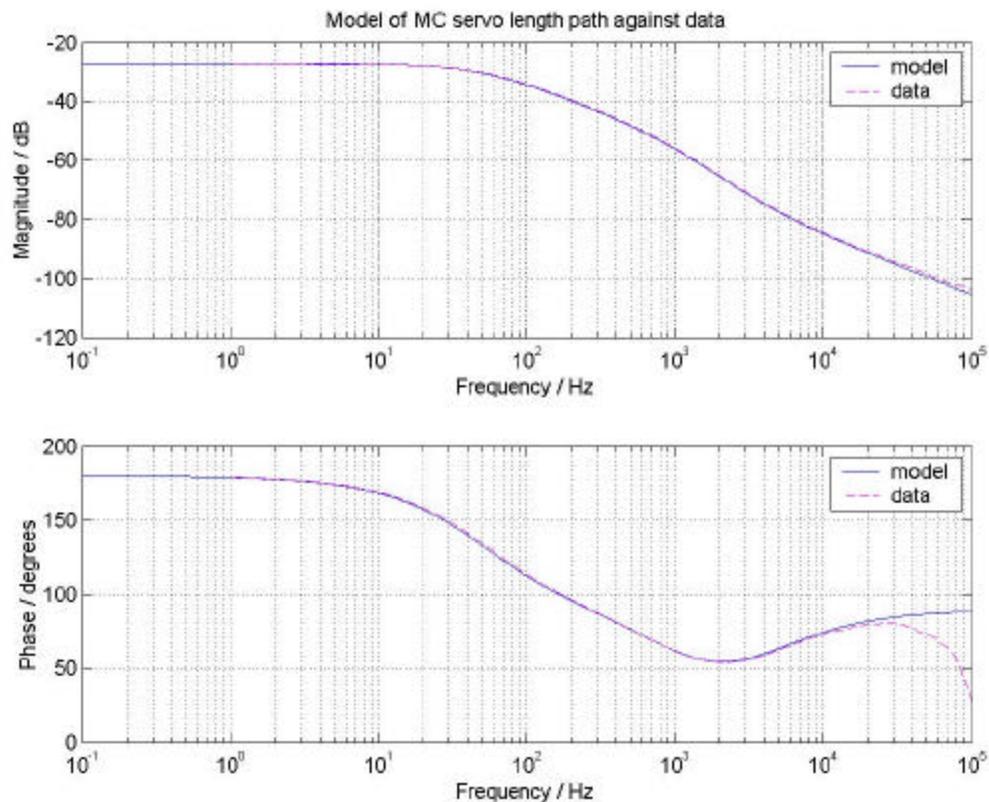


**Figure 8: A bode plot of the modeled and measured transfer functions of the length path of the MC servo.**

Figure 9 shows measured and modeled transfer functions for the path through the MC servo to the VCO, in acquisition mode. In this case the model includes block $E_{paf}$ as well as the first three poles and zeros in block $E_l$ (shown in blue) on Figure 7.

The data fits the model closely in each case. This was a puzzle since the MC servo appeared to be the part of the circuit that was preventing the mode cleaner from locking.
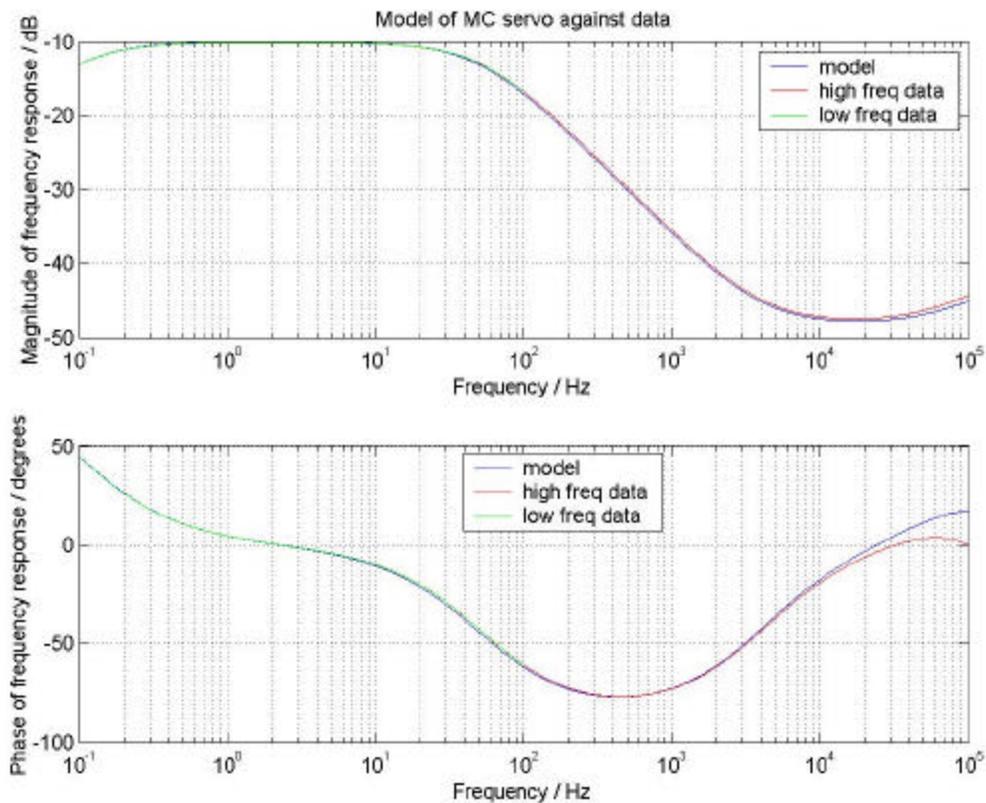
**Figure 9: A bode plot of modeled and measured transfer functions of the path through the MC servo to the VCO.**

It was found that lock could be achieved using the length path of the MC servo and an SR560 for the laser path. I measured the transfer function of the SR560 laser path for comparison with the MC servo, and the results are shown in Figure 10.

## 4.1.2 – Mirror actuator

I measured a transfer function from the input of the mode cleaner servo through to a monitoring point for one of the OSEM sensors on MC2. This includes blocks $E_m$, $E_{paf}$ and $H_m$ in Figure 7. By dividing out the MC servo TF already measured, I was able to obtain the transfer function of $E_m$ and $H_m$.

By comparing a modeled pendulum transfer function (Figure 11) with the data, I was able to estimate the quality factor of the driven damped pendulum to be of the order of 50. However, after this measurement, Ben made modifications to the satellite amplifier gains, and Ilya diagonalised the MC2 actuator[10], so the data are probably not valid. Ilya's values for the Q-factors are certainly different, although they were found by a different method. It was also later discovered that the pole-zero module had never been enabled, which would also have changed the transfer function.

20

Comparison of SR560 and MC servo transfer functions

benvco
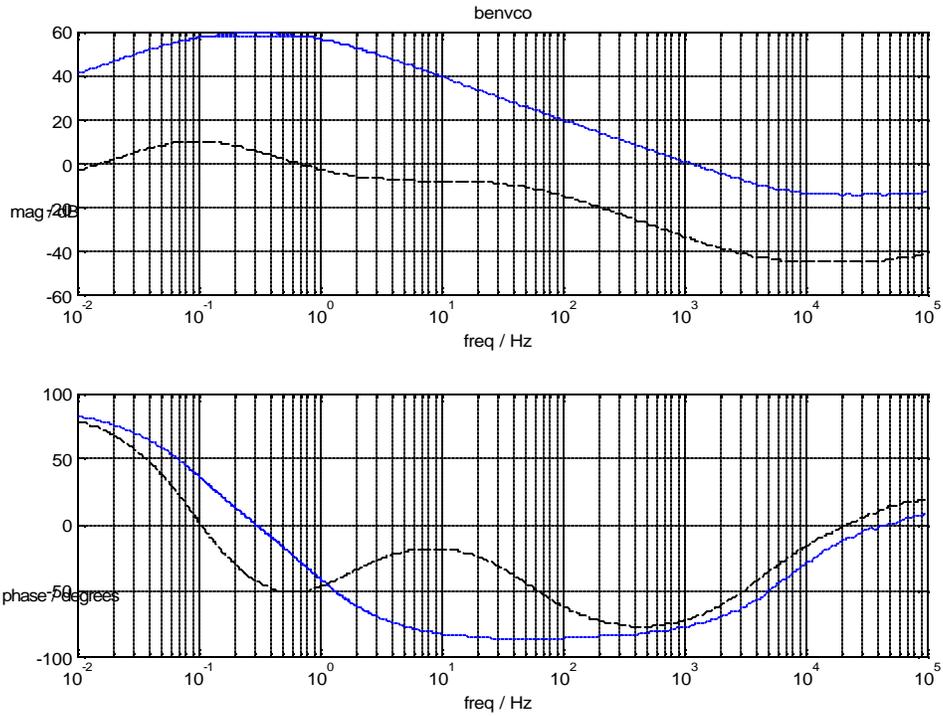


**Figure 10: A comparison between the transfer functions of the SR560 pre-amplifier set-up (blue, solid) and the MC servo path (to the VCO) that they replaced (black, dashed).**

Model of pendulum against data from MC2 and MC1 UL sensors
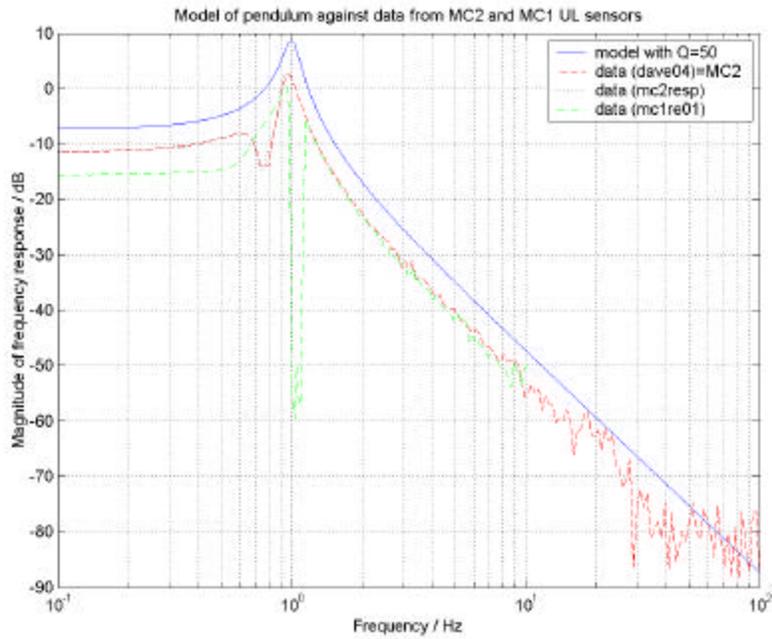


**Figure 11: The amplitude response of the transfer functions of the MC2 and MC1 mirror actuators, compared with a model damped, driven pendulum.**

On the positive side, the data for both MC1 and MC2 match the form of a damped, driven pendulum very well, and show clearly the magnitude response dying away as $1/f^2$ above the resonant frequency. This verifies the effectiveness of the pendulum design at isolating the mirror from high frequency noise.

## 4.2 – VCO measurements

I characterized the VCO at DC, by injecting a DC voltage to the "wideband input" and measuring the frequency of the response with a high frequency spectral analyzer. As can be seen in Figure 12, the response of the VCO is not perfectly linear at DC. However, for the range of voltages which should be applied when the mode cleaner is in lock (~0.5 $V_{pk-pk}$ according to page 9 of the design document[7]), the VCO appears to be linear enough (at least at DC).

**Frequency produced in the VCO output as a function of the applied voltage at the wideband input. (Error bars are too small to show.)**
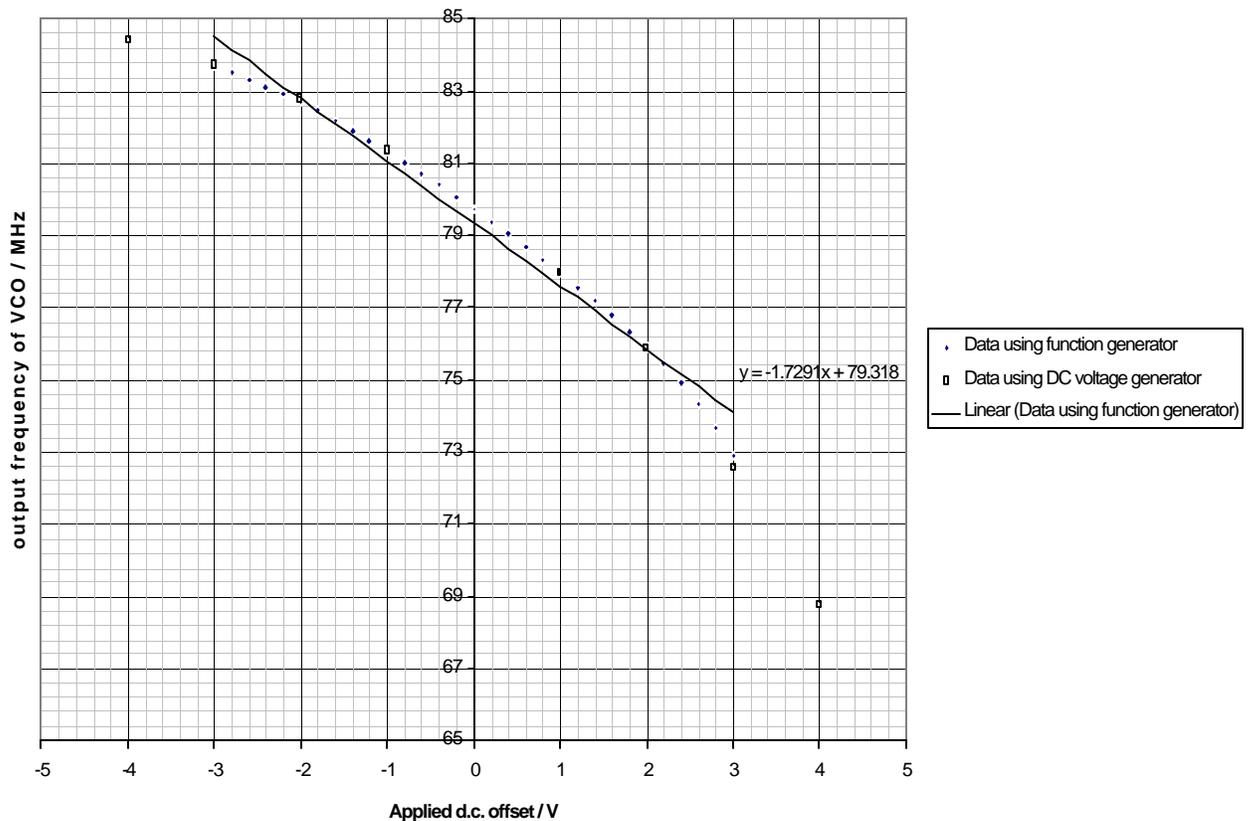


**Figure 12: Graph showing the response of the VCO to a DC signal at the wideband input.**

It should be noted that no specification exists for the tolerance of the system to non-linearities of the VCO, but the only effect of such non-linearity would be to cause the total loop gain to be dependent on the magnitude of the error signal. Since the lock of the mode cleaner should be stable over a range of loop gains it would seem reasonable to assume that small deviations from linearity are not going to pose a problem for stable operation of the system.

Measurements of the VCO response as a function of frequency (which should show a pole at 1.6 Hz and a zero at 40 Hz[12]) were extremely difficult to perform, since the frequency shift in the VCO output oscillates at the same frequency that the wideband input is driven at. The refresh rate of the network analyzer used to measure the DC response was not high enough to accurately determine the peak-to-peak frequency shift for frequencies much above 1 Hz. However, Dennis, Ilya and I did observe the magnitude of the frequency shift decrease as the frequency of the signal at the wideband input was increased above around 1 Hz, indicating the presence of a pole near this frequency.

It would be possible to test the operation of the pole-zero filter in the VCO directly by opening up the box and measuring transfer functions across just the filter part of the circuit. This would not prove that the rest of the circuitry had a flat frequency response, though. A better solution is to model the response of the whole loop, assuming the frequency response of the VCO is as designed. The fit to that model can enable the VCO response to be fully verified, since other components of the loop can be measured independently with greater ease. After I left the lab this test was carried out and the VCO circuitry was found to be faulty.

## 4.3 – Residual frequency noise in the laser beam

Using the HP3563 network analyzer, I measured the power spectrum of the error signal while the mode cleaner was locked (with SR560 pre-amplifiers instead of the MC servo). The power spectrum is shown in Figure 13.

Spikes at 60 Hz and harmonics are present, either pickup from power cables or fluorescent light flicker reaching the photodiodes. The largest peak is at 3 Hz, which is a resonance of the seismic stack on which MC1 and MC3 are mounted. There is also a large peak near 16 Hz; a frequency for which there is a notch filter on the MC servo board – disabled at the time of the measurement as it seemed to cause oscillations to build up. Above about 3 kHz, the noise seems to fall off as 1/frequency, possibly the effect of the cavity pole.

To determine the frequency noise in laser beam delivered by the mode cleaner from this spectrum, it is necessary to know the conversion factor from Volts to Hz in block $D_{mc}$ in Figure 7. I was not able to measure this for the mode cleaner in the 40m lab; the value

(11e-3 V/Hz) shown on the diagram is for the 2km interferometer at Hanford. The value for the Hanford 4km interferometer's mode cleaner is 6.5e-3 V/Hz. Since these values are so similar, I will assume (rashly) a value of the same order for the 40m lab, i.e. $\sim 10^{-2}$ V/Hz. Based on this value, I have approximately sketched the frequency fluctuation requirement in red on Figure 13.
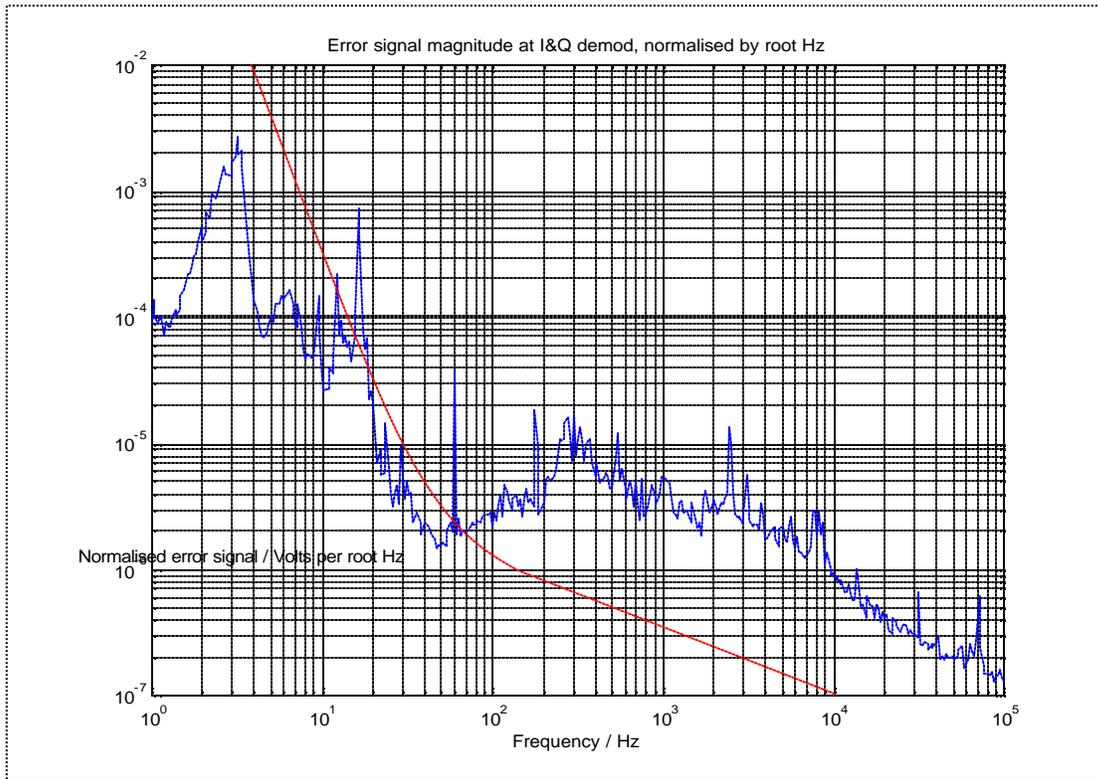


**Figure 13: Power spectrum of the demodulated error signal (blue) with an estimate (red) of the level required to meet the frequency fluctuation requirements.**

Clearly, if my assumption is at all valid, the frequency noise in the mode cleaner output was an order of magnitude higher than specification at frequencies from $10^3$ to $10^4$ (which are certainly in the detection band for gravitational waves) when I measured it. At that time, increasing the gain of the SR560 pre-amplifiers processing the error signal caused the mode cleaner to lose lock, offering little prospect to reduce this noise. However, it is important to remember that the mode cleaner was not operating in its designed configuration.

## 4.4 – Storage time and finesse of mode cleaner

With the mode cleaner locked (using the set up described at the start of the section), Osamu and I attempted to measure the ringdown of the mode cleaner. This is the decay

of the transmitted light as a function of time, $t$, when lock is suddenly lost, taking the form $I = I_0 e^{-t/t}$ , where $I$ is the transmitted intensity and $t$ is the cavity storage time.
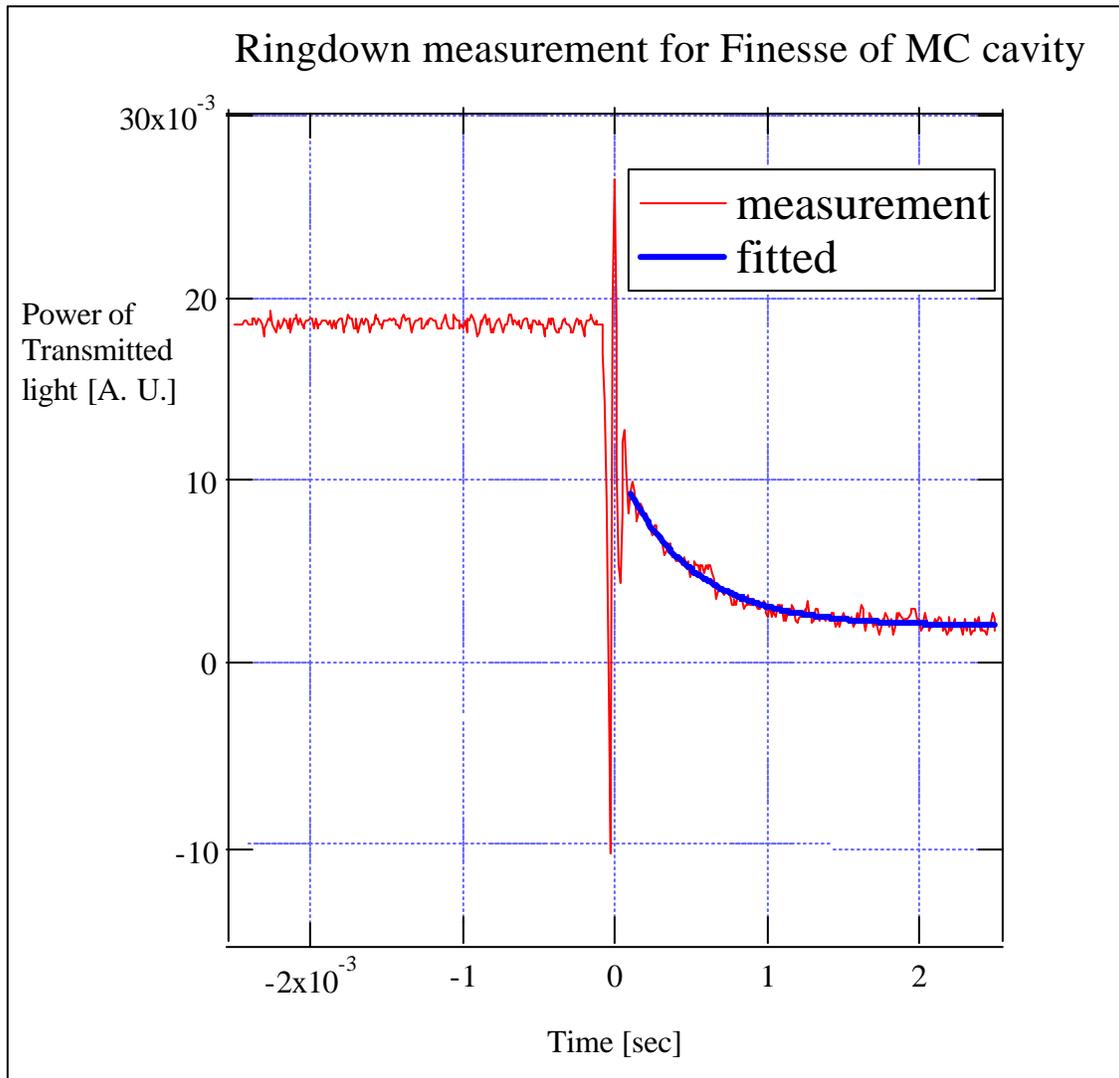


**Figure 14: A graph of the mode cleaner transmitted light as a function of time (red) with a fitted exponential decay (blue).**

The most obvious method was to interrupt the laser beam at a point before it was passed to the mode cleaner. However, the only method available to us at the time was to quickly cut the beam with a beam block. When the transmitted light photodiode was monitored on an oscilloscope, this method did not produce the expected exponential decay in the intensity, indicating that our beam interruption was not fast enough.

As an alternative to blocking the beam, Osamu used the "reset" button on one of the SR560 pre-amplifiers to knock the mode cleaner out of lock. Figure 14 shows a plot of the ringdown produced when the lock was interrupted. Fitting a decaying exponential

gives a storage time of $(46.8 \pm 1.4)$ **ms**. This storage time is equivalent to a finesse of $1630 \pm 49$, or a cavity pole of $(3400 \pm 100)$ Hz.

## 4.5 – Intensity stability

A fast photodiode was placed in the beam transmitted by the mode cleaner. The power spectrum of its output (in Volts) was measured using the HP3536. To normalize this spectrum, the data were divided by the mean voltage output of the same photodiode. The results, normalized by root Hz, are shown in Figure 15.
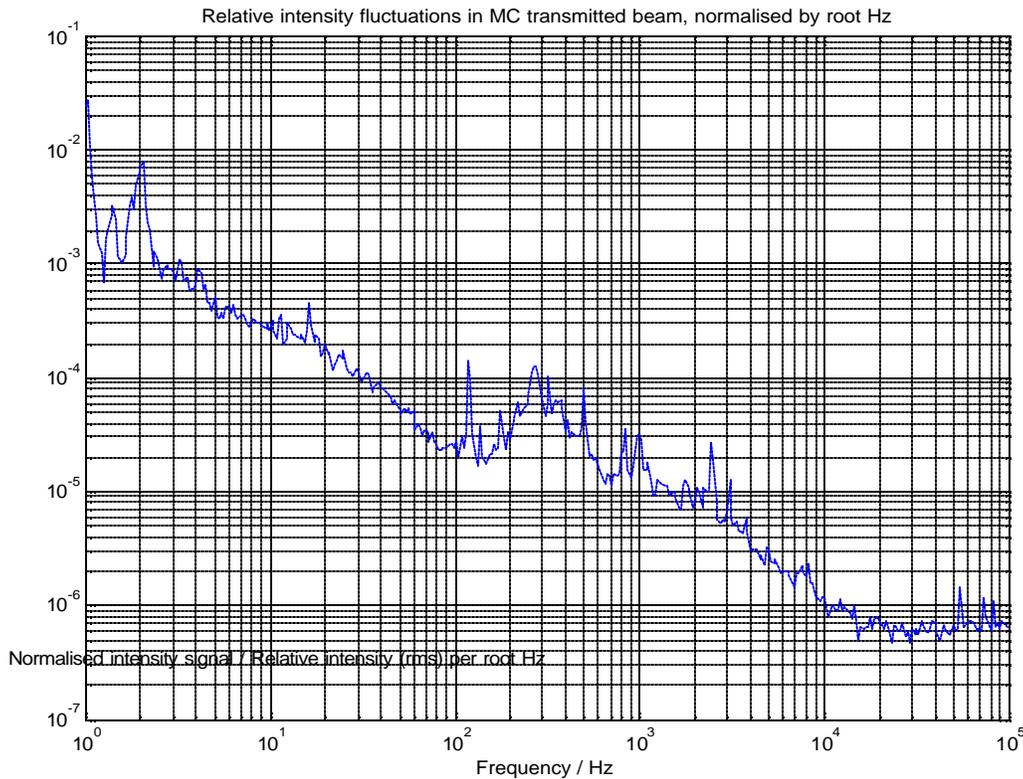


**Figure 15: A power spectrum of the intensity fluctuations on the beam passed by the mode cleaner, normalized by root Hz.**

The requirement for power fluctuations just before the power recycling mirror (i.e. after the mode cleaner) is $10^{-8}$ per root Hz from 100 Hz to 10 kHz[13]. The data I obtained show the mode cleaner to pass light which has noise about 3 orders of magnitude above this. However, the intensity stabilization servo is yet to be installed.

The intensity fluctuations of the mode cleaner transmitted beam are compared in Figure 16 with those previously measured[14] at a point just after the PSL's pre mode cleaner. Surprisingly, the fluctuations in the MC transmitted beam appear to be greater in magnitude than those in the beam from the PMC. They do not suffer from the same

strange sawtooth pattern that had been previously observed, suggesting that this may have been an artifact of the measurement process.

**Unnormalised intensity fluctuations of mode cleaner transmitted beam**
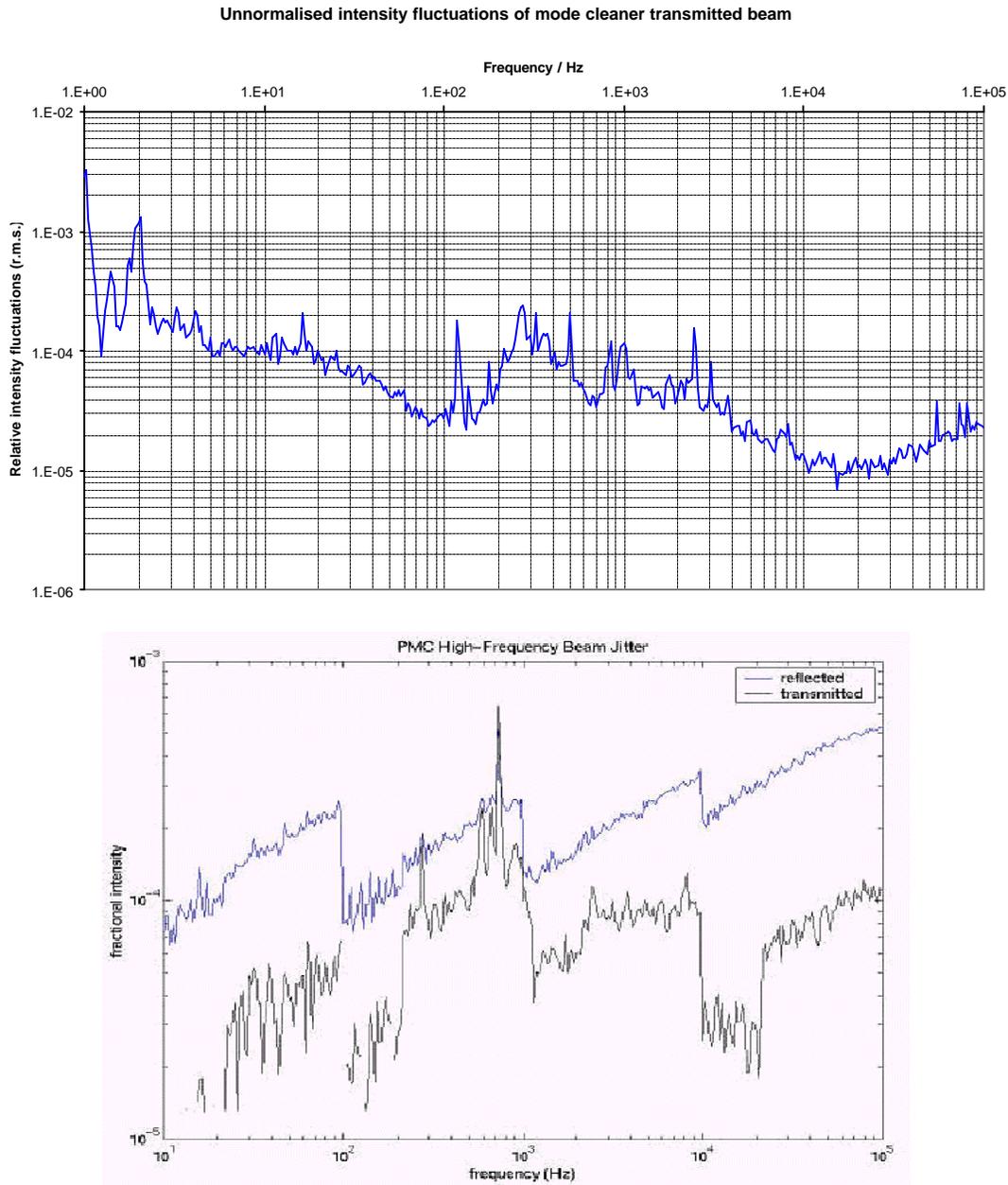


**Figure 16: Unnormalized intensity fluctuations (top) in the beam delivered by the mode cleaner, for comparison with previous measurements (bottom) of the beam delivered by the PSL.**

It seems strange that the intensity fluctuations should be greater at a point after the mode cleaner than before it. It is possible that the measured power spectrum is also affected by the position stability of the beam, since the photodiode used had a small surface area and the beam diameter was about twice as large in my measurement. The position stability,

whilst not measured, may well have been poor since there had been problems with the actuation of MC1 (demonstrated by its failure to be diagonalised[10]) that would have reduced the effectiveness of its damping.

## 4.6 – Transverse beam profile

With Osamu's assistance, I used a Photon, Inc. device called BeamScan to determine the transverse profile of the beam, as shown in Figure 17.
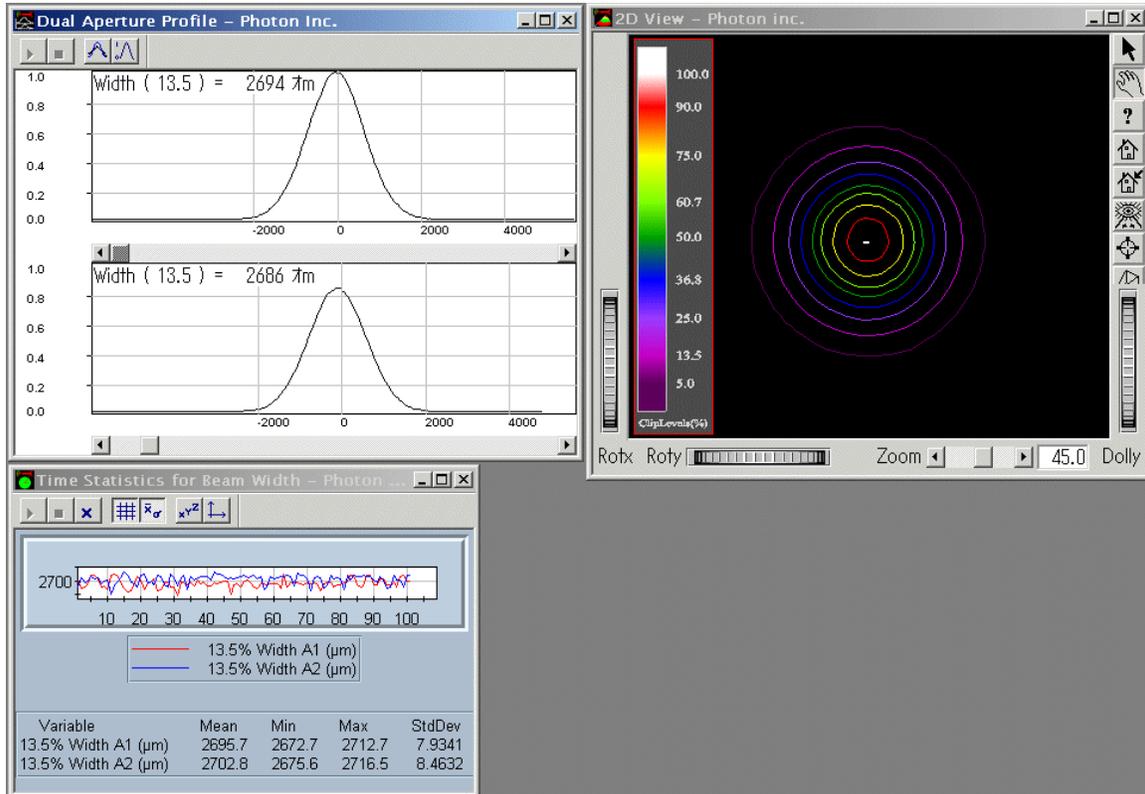


**Figure 17: Screenshot from the software used with the BeamScan to measure the transverse profile of the mode cleaner transmitted beam.**

The ellipticity, $e$, of the beam is defined as

$$e = 1 - \frac{b}{a}$$

where $a$ and $b$ are the semi-major and semi-minor axis lengths respectively. The BeamScan data gives an ellipticity of 0.3 % for the beam passed by the mode cleaner.

## 4.7 – Visibility

The alignment of the cavity was adjusted to maximize the transmitted light intensity with the mode cleaner in lock. The mode cleaner reflected light photodiode was connected to an oscilloscope. The voltage on the scope was then measured for the locked mode cleaner (giving a measure of the minimum power reflected by the cavity). The mode cleaner was then unlocked. The voltage corresponding to the maximum reflected power was measured.

The visibility was then calculated using the formula in section 3.2.9, i.e.

$$V = \frac{2.72 - 0.292}{2.72 + 0.292}$$
$$= 0.806$$

This is substantially less than the calculated value in 3.2.9. That value assumes perfect mode matching, alignment, etc. and most importantly does not take the modulation of the light into account. I do have a reservation about the reliability of the measurement, in that I did not check the voltage produced by the photodiode with the laser beam blocked.

## 4.8 – Length of mode cleaner

The length of the mode cleaner was measured (after I left the lab) using a resonant sideband placed on the carrier light using a Pockels cell. The mode cleaner was first locked, to ensure that the carrier light (whose frequency is precisely known) was resonant. The frequency of the phase modulation was then varied until it too was resonant in the cavity.

Resonance was shown by demodulating the light reflected from the mode cleaner at the same frequency as the modulation. When the demodulated signal fell to a minimum (close to zero), the sideband could be said to be resonant. Figure 18, taken from the lab's electronic log[15], shows the well-defined minimum in the demodulated signal. The length was measured to be $(13.5467 \pm 0.0001)$ m.

# MC length measurement



Transmitted frequency $f_0$=33195400 +- 50 Hz
Length of MC Lmc=3c/(2 $f_0$) =13.5467 m +- 20 $\mu$m
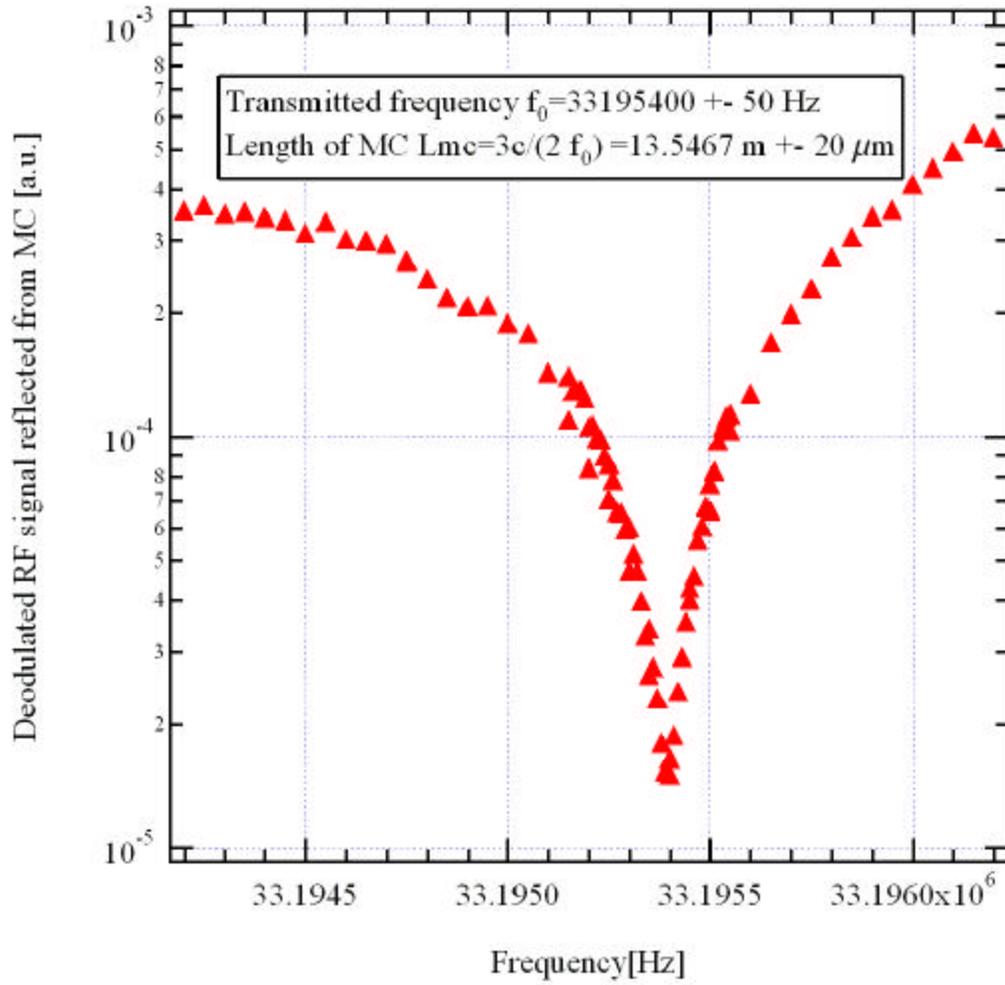
**Figure 18: Graph showing the demodulated reflected light signal as a function of the modulation/demodulation frequency. The sharp dip indicates resonance of the sideband in the mode cleaner.**

# 5 – Additional tasks performed

## 5.1 – QPD readouts to EPICS

The lab currently has four quadrant photodiodes (QPDs) that will eventually all be used to monitor the alignment in position and angle of the beams exiting the PSL and mode cleaner. In order that the outputs of these devices could be more easily monitored while they were used generally for alignment tasks, I designed the screen shown in Figure 19. This screen was made using the software platform used by all of the LIGO control interfaces; EPICS (Experimental Physics Industrial Control System).
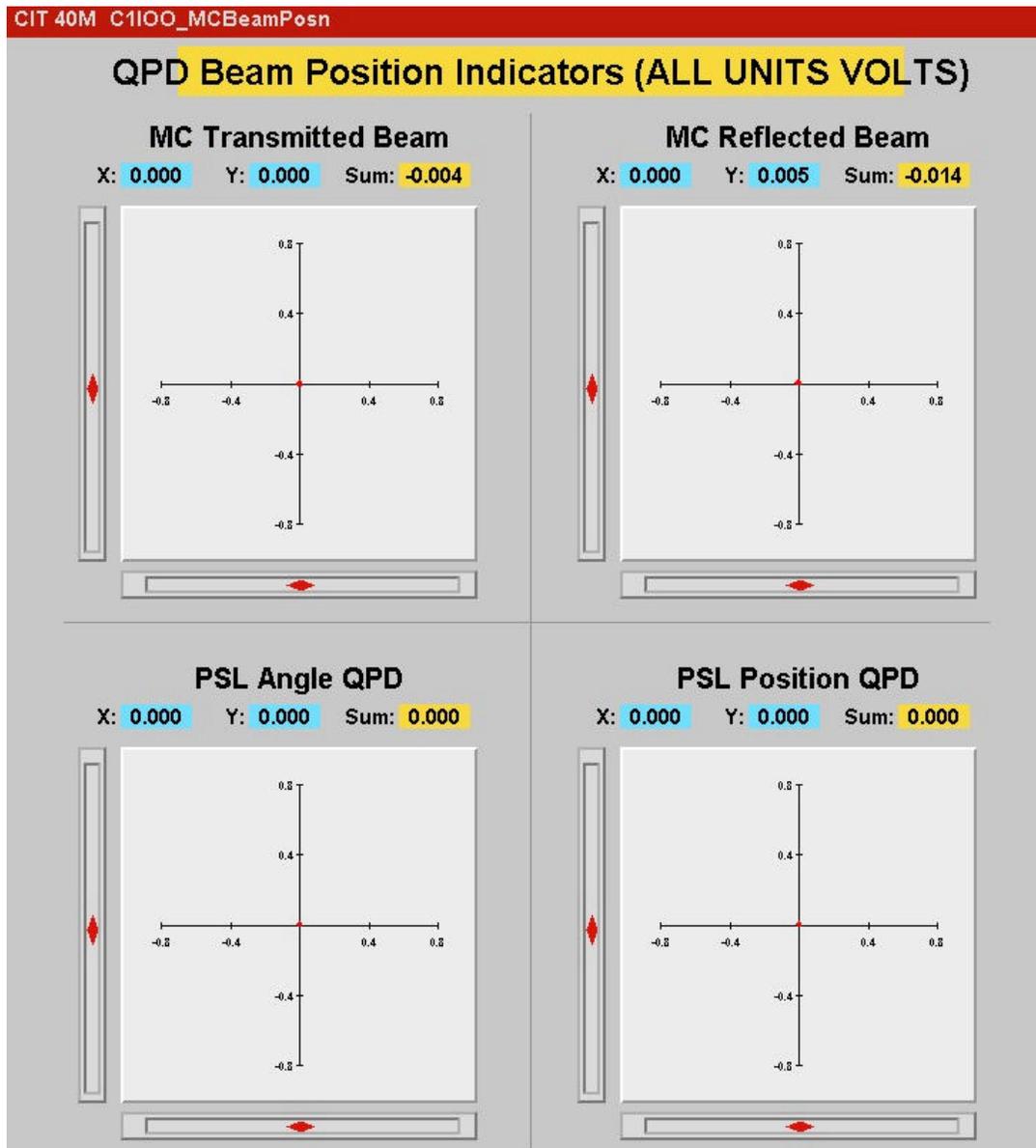


**Figure 19: EPICS screen for QPD readout.**

## 5.2 – Pole-zero module controller (EPICS)

When it was noticed that the pole-zero module (a filter in the length control path of the mode cleaner) was not enabled, I built a simple screen (shown in Figure 20) in EPICS to turn on each filter.
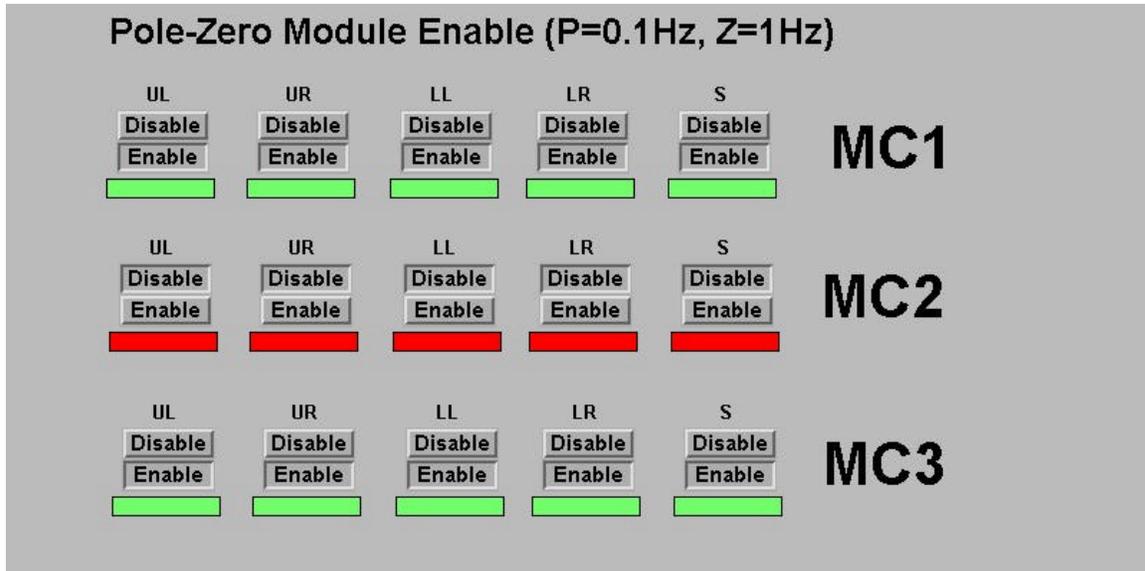


**Figure 20: EPICS screen to enable pole-zero modules.**

# 6 – Results, Discussion and Conclusions

## 6.1 – Summary of results

During the summer, I performed or assisted with the measurements documented in section **4**, whose results are listed below:

(i)     The measured transfer functions of the MC servo board closely matched models based on the circuit diagrams.

(ii)    The response of the mirrors to signals fed to the actuators matched a model for a damped, driven pendulum with a Q of the order of 50.

(iii)   The response of the VCO was 1.7 MHz per volt, approximately linear over its operating range.

(iv)    The Finesse of the cavity is $1630 \pm 49$.

(v)     The residual frequency noise was probably an order of magnitude higher than specification for frequencies from 100 to 1000 Hz when the SR560s were used in place of the MC servo.

(vi)    The intensity stability of the beam delivered by the mode cleaner was 3 orders of magnitude worse than it needs to be. However, the intensity stabilization servo is not yet installed.

(vii)   The transverse profile of the beam appears highly circular. Ellipticity is only 0.3%.

(viii)  The visibility of the cavity is 0.806

(ix)    The length of the mode cleaner is $(13.5467 \pm 0.0001)$ m


## 6.2 – Discussion

## 6.2.1 – The control system

Although measuring transfer functions occupied a good deal of my time, they were probably not as useful as they could have been. This is because I was comparing the measurements with models based on circuit diagrams rather than theoretical considerations of the desired responses; particularly unhelpful when a number of the circuit diagrams later turned out to have been wrong. The reason that theoretical models weren't used was that I knew only what the response of the entire control loop was meant to be and not how each component made that happen. As far as I could determine there were no documents containing these details and the persons who designed the system weren't available to me.

The direct measurements made of the VCO were useful in determining the conversion factor from voltage to frequency. This has been specified on a number of occasions, but not consistently, and can be found listed as 0.5, 1 and 2 MHz per Volt in different documents. The measurement failed to find the faults in the VCO that prevented the system locking, but without up-to-date circuit diagrams this was always going to be very difficult.

Measurements of the effects of forcing lock of the mode cleaner using SR560 pre-amplifiers rather than the MC servo board delivered relatively promising results. If my estimate of the relation between the error signal and the laser frequency noise is valid, and the noise in the beam from the PSL is as specified, then even this fragile lock was able to cause at least 40 dB of noise suppression. (This is because I estimated the error signal to be one order of magnitude (20 dB) too large, and the design states that the mode cleaner will need to provide 60dB of suppression to meet spec.

At this time the mode cleaner optics' suspensions were not properly diagonalised to decouple translation from pitch and yaw. One would expect this to be detrimental to the ability of software to properly damp their motion, and it may have forced the use of lighter damping than would be ideal.

The intensity stability measurement may prove a useful baseline as the intensity stabilization servo is installed, although proper diagonalisation of the optics may improve the positional stability of the beam and have a knock-on effect on intensity stabilization (or at least the perception of it by a small-aperture, fixed-position photodetector).

## 6.2.2 – Optical properties of the mode cleaner

Although the optical properties measured were done so in a rather fragile state of lock, they were still useful as a check on the mode cleaner optics.

The finesse seems unlikely to change dramatically in the course of future modifications to the system. However, a more accurate measurement could be made by using an electro-optic shutter to turn off the beam being supplied to the mode cleaner. This would be able to cut off the beam in nanoseconds and provide better ringdown data.

The low ellipticity of the beam is probably a sign that the non-$TEM_{00}$ modes are highly suppressed, as desired. The ellipticity of the beam from the PSL when it was commissioned was 2.7 %. Since then, however, Aya has worked on improving the fit of the beam profile to mode-matching models that specify its diameter [16]. I do not have data for the ellipticity of the beam as it exits the PSL, so I cannot say whether the beam is more circular after the mode cleaner or before it.

The cavity visibility measurement is affected by a number of factors, including the alignment of the mode cleaner, the degree of mode matching, the modulation depth of the non-resonant sidebands, the transmittances of the mirrors and the losses in the mode cleaner. Several of these are unknown, so it is difficult to make useful quantitative conclusions from the visibility value. Future improvements in factors like alignment and mode matching can be quantified, however, using the visibility as a measure.

The length of the mode cleaner is less than 4 mm longer than design. Although I do not know quantitatively how this will affect values such as the *g*-factor of the cavity, it seems likely that such a small variation (around 0.03 %) will have a negligible effect.

## 6.3 – Conclusions

(i)     The control system as designed didn't work well enough to lock the mode cleaner while I was working in the lab.

(ii)    It was possible to lock the mode cleaner by replacing part of the loop (MC servo) with a more flexible filtering and amplification stage (SR560 pre-amps), suggesting that the main fault was in the signal conditioning and not the optics/sensors/actuators.

(iii)   Locking with SR560s reduced the noise in the laser sufficiently, given the problems encountered, to suggest that when the system works properly the design specification for frequency noise suppression can be met.

(iv)    We have a baseline for future measurements of intensity stability.

(v)     The finesse of the cavity is as specified, as far as can be determined by the current precision of measurement.

(vi)    The beam passed by the mode cleaner has a highly circular Gaussian transverse intensity profile.

## 6.4 – Further Work

- When all problems with mode cleaner electronics are fixed and all suspensions are diagonalised, the total closed loop transfer functions should be measured. They can then be compared to design specifications for the unity gain frequency, phase margin and crossover frequency between the servos to the laser and the mirror.

- The frequency noise in the laser should be measured to ensure that it is within specification.

- The intensity stability servo can be installed and the improvement in intensity stability measured.

- If the transverse profile of the beam is measured before it enters the mode cleaner it will be possible to determine the effect of the mode cleaner on the transverse modes of the beam.

- Using an electro-optic shutter, the finesse of the cavity can be measured to a higher precision.

## *7 – Acknowledgements*

# 8 – References

[1] http://www.ligo.caltech.edu.

[2] A. Abramovici, et al., *LIGO: The Laser Interferometer Gravitational-Wave Observatory*, Science **256** (1992) 325.

[3] See, for example, LIGO-G020229-00 – the *Advanced LIGO Input Optics Design Requirements Review* presentation.

[4] B. Abbott, G. Billingsley, L. Jones, R. Karwoski, J. Romie, M. Smith, D. Ugolini, S. Vass, A. Weinstein, *Conceptual Design of the 40 meter Laboratory Upgrade for prototyping an Advanced LIGO Interferometer*, LIGO-T010115-00-R – an internal working note of the LIGO project.

[5] A.J. Weinstein, *The Physics of LIGO: Lecture*, LIGO-G000164-00-R – an internal working note of the LIGO project.

[6] E. Black, *Notes on the Pound-Drever-Hall technique*, LIGO-T980045-00-D – an internal working note of the LIGO project.

[7] P. Fritschel, N. Mavalvala, D. Ouimette, *Mode Cleaner Length/Frequency Control Design*, LIGO-T970218-02-D – an internal working note of the LIGO project.

[8] S. Kawamura, J. Hazel, *Small Optics Suspension (SOS) Final Design (Mechanical System)*, LIGO-T970135-02-D – an internal working note of the LIGO project.

[9] J. Heefner, R. Bork, *Digital LOS and SOS control systems for LIGO*, LIGO-T000073-00-C – an internal working note of the LIGO project.

[10] I. Berdnikov, *Characterization and commissioning of digital suspensions for the 40m mode cleaner*, Final SURF report (2002).

[11] M. Mohana, *Mode Cleaner Servo* circuit diagram, LIGO-D000347-B – an internal working note of the LIGO project.

[12] R. Abbott, *PSL 80 MHz VCO*, LIGO-D980401-B-C – an internal working note of the LIGO project.

[13] P. King, S. Savage, R. Seel, *(Infra-red) Pre-stabilised Laser(PSL) Design Requirements*, LIGO-T970080-09 – an internal working note of the LIGO project.

[14] D. Ugolini, P. King, R. Abbott, B. Abbott, S. Vass, A. Weinstein, *LIGO Caltech 40-Meter PSL Commissioning Report*, LIGO-T010145-00-D – an internal working note of the LIGO project.

[15] http://www.ldas-sw.ligo.caltech.edu/ilog/pub/ilog.cgi?group=40m (09/12/02) – LIGO 40m lab electronic log (password required).

[16] A. Sekido, *Measurement of the laser beam profile at the 40 Meter Prototype Interferometer*, LIGO-T020143-00-R – an internal working note of the LIGO project.